Computational and Theoretical Chemistry 1027 (2014) 135–141

Contents lists available at ScienceDirect

Computational and Theoretical Chemistry

journal homepage: www.elsevier.com/locate/comptc

Alkylation of guanine by formononetin nitrogen mustard derivatives: A DFT study

Sourab Sinha, Pradip Kr. Bhattacharyya *,[1]

Department of Chemistry, Arya Vidyapeeth College, Guwahati, Assam 781 016, India

ARTICLE INFO

Article history:
Received 1 October 2013
Received in revised form 5 November 2013
Accepted 5 November 2013
Available online 16 November 2013

Keywords:
DNA alkylation
DFT
Aziridinium ion
MEP
MHP
Formononetin

ABSTRACT

We studied the thermodynamic and kinetic aspects of guanine alkylation by five derivatives of formononetin nitrogen mustard using density functional theory (DFT). Investigation of the reactivity pattern of the aziridinium ion intermediates as well as drug-guanine adducts were performed using Density functional reactivity theory (DFRT). Aziridinium ion formation was observed to be endothermic, in contrast, the drug-guanine adduct formation was exothermic. A significant interaction of the aziridinium ion with guanine has been observed. The results illustrate the applicability of maximum hardness principle (MHP) and minimum electrophilicity principle (MEP).

1. Introduction

Bis-alkylating nitrogen mustards are the earliest and perhaps the most extensively studied and clinically employed DNA interstrand cross-linking agent, exploited to treat cancer since its invention in the early twentieth century [1–7]. Mode of action of these drug molecules is well comprehended and previous experimental studies confirmed that its cytotoxicity is allied with its alkylating ability by means of reaction with biomolecules, preferentially at nucleophilic centres in DNA bases [8–12]. These drug molecules form a very reactive positively charged intermediate, the aziridinium (Az^+) ion and preferential alkylation at the endocyclic nitrogen and exocyclic oxygen centres of DNA bases is the suggested mechanism [13–16]. Earlier works confirmed that out of different nucleophilic sites in DNA bases, N7 of guanine is the most nucleophilic one and was shown to be a highly preferred site over others for alkylation [17,18]. During alkylation, each of the chloroethyl side chains of the nitrogen mustard (a) spontaneously cyclizes to form Az^+ ion (b) that finally binds to DNA (at N7 of guanine), resulting a mono-adduct (c) [13,19–21], Fig. 1.

Mustine (R = $-CH_3$ in Fig. 1) is highly reactive and prone to hydrolysis; it also reacts immediately with the nucleophilic centres in biomolecules. Because of its high affinity towards water molecules, it is marketed as a dry solid and when required, its aqueous solution is prepared just prior to injection. Therefore, more stable analogues were sought. Substitution of the methyl group on the N-atom of mustine by aryl conjugate groups make the N-atom less nucleophilic and slow down the rate of Az^+ ion formation [22]. This decreases the reactivity of the nitrogen mustard and as a result of this stabilization some of the drugs can be administered orally [22]. In last few decades, a number of such drugs have been synthesized and their cytotoxicity has been tested [23–28]. Recently, Ren et al. synthesized a series of derivatives of formononetin nitrogen mustard, many of them exhibiting promising anticancer activity [28].

Understanding the kinetic as well as thermodynamic aspects of guanine alkylation by nitrogen mustards drew attention of researchers and a number of computational studies have been carried out in recent years [18,29,30]. Mann from his explicit study on the formation of Az^+ ion of nitrogen mustards using ab initio dynamics confirmed a concerted nucleophilic displacement reaction involving simultaneous dissociation of the C–Cl bond and internal cyclization of the Az^+ ring [29]. Polavarapu et al. studied thermodynamic and kinetic driving force involved in alkylation of guanine for three clinically used nitrogen mustards [30].

In recent years, among different computational methods, density functional theory (DFT) became one of the best choices for thermodynamic and kinetic studies of chemical and biochemical reactions [31]. Global and local reactivity descriptors defined under DFRT are the most preferred theory in elucidation of reactivity pattern in a molecular system as it bears a simple conceptual

* Corresponding author.
E-mail addresses: sourabsinha39@gmail.com (S. Sinha), prdpbhatta@yahoo.com (P.Kr. Bhattacharyya).
[1] http://www.pkb-chem.co.in

2210-271X/$ - see front matter © 2013 Elsevier B.V. All rights reserved.
http://dx.doi.org/10.1016/j.comptc.2013.11.003

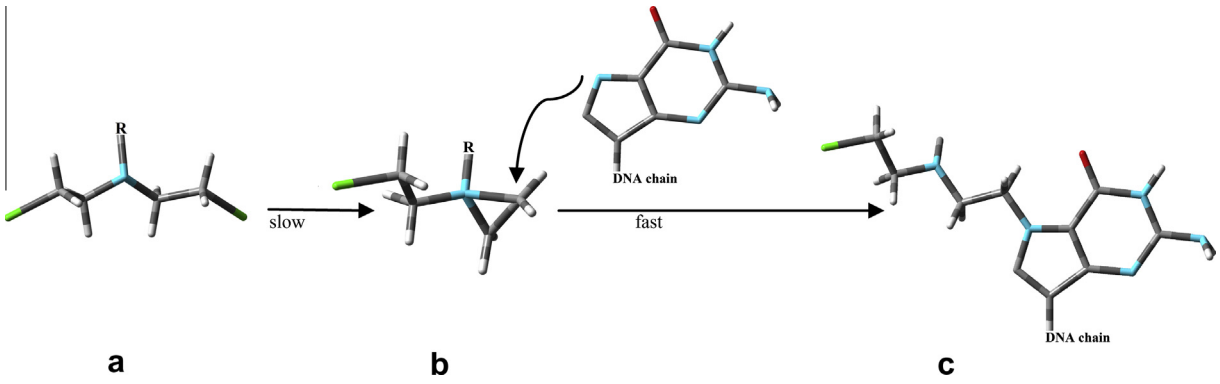

Fig. 1. Mechanism of guanine alkylation by nitrogen mustard.

framework and is computationally tractable. Wide applicability of these descriptors is well documented [32,33]. Global reactivity descriptors (GRD) such as global hardness and global electrophilicity index are employed to measure the overall reactivity of a chemical species and are in extensive use by the researchers [34–37].

In our present investigation, we have considered five derivatives of formononetin nitrogen mustard, based on their lower IC_{50} values, synthesized by Ren et al. [28], Table 1, and used DFT to study thermodynamic and kinetic aspects of alkylation of guanine and DFRT to monitor the reactivity of the intermediates and drug-guanine adducts formed by these drugs.

2. Theoretical details of reactivity descriptors

In DFT, chemical potential (μ) and global hardness (η) are defied as the first and second derivative of energy with respect to the number of electrons respectively [38–40]. Use of finite difference approximation and Koopmans' theorem [41] leads to the working formulae for μ and η as:

$$\eta = \frac{\varepsilon_{LUMO} - \varepsilon_{HOMO}}{2} \tag{1}$$

$$\text{and} \quad \mu = \frac{\varepsilon_{LUMO} + \varepsilon_{HOMO}}{2} \tag{2}$$

Parr and co-workers proposed global electrophilicity (ω) as a measure of electrophilic power of a ligand and its propensity to soak up electrons in terms of chemical potential and chemical hardness as [37]:

$$\omega = \frac{\mu^2}{2\eta} \tag{3}$$

3. Computational details

The geometrical minima of the species were optimized using polarized basis set 6-31+G(d,p) with Becke three parameter exchange and Lee, Yang and Parr correlation functional, B3LYP [42,43]. Vibrational frequency analysis was performed in all cases to ensure that the reactants and products have no imaginary frequency. Calculation of the transition state (TS) structure was performed using QST3 method [44] and its genuineness was confirmed by an imaginary frequency of the vibrational mode. Interaction energies (ΔE_{int}) were calculated using super molecular approach [for $A + B \rightarrow AB$, $\Delta E_{int} = (E_{AB}) - (E_A + E_B)$, where, E is the total energy of the corresponding species]. Global reactivity descriptors (global hardness, chemical potential and global electrophilicity) were calculated using Eqs. (1)–(3). Solvation energies were calculated using self-consistent reaction field (SCRF) approach with Polarizable Continuum Model (PCM) [45]. Solvation studies were performed on the gas phase optimized geometries at di-electric constant, $\varepsilon = 78.35$ for aqueous phase. The free energy of solvation (ΔG_{sol}) of the species was computed using SMD solvation model proposed by Truhlar and coworkers [46]. All calculations were performed using Gaussian09 [47].

4. Results and discussion

4.1. Activation of the drug: the aziridinium ion formation

As illustrated in Fig. 1, the first step of the drug activation mechanism involves the release of the chloride ion from the drug molecule, thus forming an Az^+ ion. The second step of the mechanism comprise of interaction of the N7 site of guanine with the C1 (numbered arbitrarily) centre of the Az^+ ion, finally forming the drug-guanine adduct. The path followed by the drug molecules to form Az^+ ion involves a transition state (TS1) which was confirmed by earlier studies performed on some other nitrogen mustards [8–13,19–21]. To understand the kinetic and thermodynamic aspects of Az^+ ion formation reaction, we followed the reaction pathway and calculated the free energy of activation and enthalpy of the reaction. A schematic diagram of TS1 is presented in Fig. 2.

It is important to note that the structural parameters in TS1 are nearly equal in all cases; with C1–N3 bond lengths ~1.5 Å, C1–Cl bonds lengths ~2.8 Å and ∠N3C2C1 bond angles are in the range 62–54°, on the other hand, the structural geometry of the drug molecules are, C1–N3 bond lengths are ~2.4 Å, C1–Cl bonds lengths are ~1.81 Å and ∠N3C2C1 bond angles are ~109°. As the reaction progresses, the ∠N3C2C1 bond angle reduces; simultaneous dissociation of C1–Cl bond and internal cyclization of the trycyclic Az^+ ion takes place. Values of the ∠N3C2C1 bond angle indicates that around the TS1, formation of Az^+ ion is almost completed. Earlier ab initio dynamics study reported a shorter C1–Cl bond length (2.37 Å) at the TS in case of mustine [29]. Among the chosen set of drug molecules, the parent molecule formononetin (1 in Table 2), exhibits a free energy of activation of magnitude 44.72 kcal/mol in gas phase which reduces to 19.58 kcal/mol in aqueous phase, Table 2.

Rest of the molecules also showed a free energy of activation of almost the similar magnitude. A spiky reduction of the free energy of activation in aqueous phase bears importance since the reaction takes place in cytoplasm (a polar medium). Values obtained in aqueous phase guaranteed a sturdy role of the polar solvent on the energy barrier, and we expect faster Az^+ ion formation in cytoplasm compared to gas phase. Enthalpy values show that Az^+ ion formation is endothermic in nature in both the phases. The observed gas phase enthalpies are ~126 kcal/mol; however, in

Table 1
Formononetin nitrogen mustard derivatives considered for study.

Entry no.	
	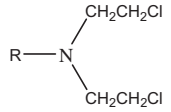 Nitrogen mustard
1	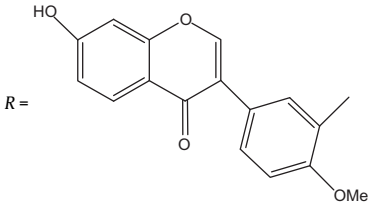
2	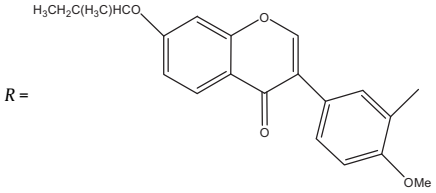
3	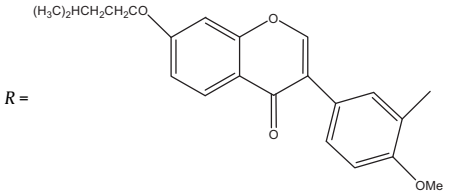
4	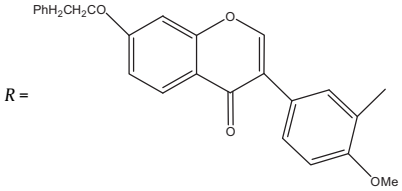
5	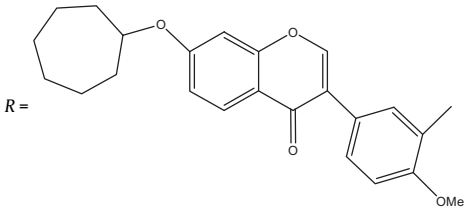

contrast, an insightful decrease in the enthalpy values in aqueous phase (~17 kcal/mol) is observed, Table 2.

Our results attested the role of solvent on free energy of activation as well as enthalpy of the reaction. Earlier, Polavarapu et al. established that, for mustine, the process of Az^+ ion formation is exothermic where as in case of chlorambucil and melphalan, consisting of aromatic groups at N3, the reaction is endothermic [30]. Being a charged species, the stability of Az^+ ion is pitiable and we observed the enthalpy of the reaction to be quite high, however, addition of polar solvent (water) reduces enthalpy of the reaction. Positive enthalpy of formation of Az^+ ion, a → b, implies thermodynamic instability of the Az^+ ion.

Reactivity of the drug molecules is expected to influence the Az^+ ion formation reaction and hence reactivity of the drug molecules stands importance; accordingly the reactivity pattern of the drug molecules in terms of global hardness (η) and global philicity (ω) were examined in both phases. Moreover, reactivity of the Az^+ ions is important for the second step, the adduct formation. Plots of η and ω of the drug molecules (Fig. 3(i and ii) and Az^+ ions (Fig. 3(iii and iv) in gas and aqueous phases are presented in Fig. 3. Among the chosen set of drug molecules, 2a and 5a showed maximum hardness (lower reactivity, in accordance to maximum hardness principle, MHP) and 1a shows minimum hardness (highest reactivity) in gas as well in aqueous phases, Fig. 3(i and ii). Important to note is that reactivity pattern is not affected by introduction of solvent phase.

The maximum hardness principle (MHP) [48,37] and minimum electrophilicity principle (MEP) [49] are widely accepted basic principles of chemical reactivity. In our earlier works too, these principles were applied successfully; application of external electric field on Az^+ ions of mustine [50] and during its structural variations [51]. In present case too, these two principles showed their consistency in both phases. Thus, being with MHP, we may expect that tendency to form Az^+ ions will be maximum for 1a. Fig. 3(iii and iv) presents the hardness and electrophilicity of the corresponding Az^+ ions (1b–5b). Reactivity pattern of Az^+ ions is similar

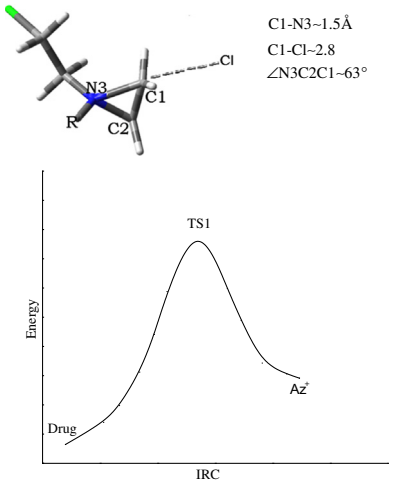

Fig. 2. Schematic diagram of the transition state involved in aziridinium ion formation (TS1, a → b).

Table 2
Free energy of activation ($\Delta G_1^{\dagger}$) and change in enthalpy (ΔH_1) involved in Az^+ ion formation in gas and aqueous phase (values are in kcal/mol, '*a*' denotes the drug molecules and 'b' denotes the Az^+ ions).

Step	$\Delta G_1^{\dagger}$		ΔH_1	
	Gas phase	Aqueous phase	Gas phase	Aqueous phase
1a → 1b	44.72	19.66	127.78	17.29
2a → 2b	43.32	20.69	126.78	17.34
3a → 3b	43.44	21.90	126.97	16.76
4a → 4b	43.74	20.23	126.81	17.37
5a → 5b	43.55	20.86	126.66	17.35

to that of their corresponding drug molecules (1a–5a). Importantly, 1b shows minimum hardness and accordingly is expected to be most reactive. On the other hand, 2b has the maximum hardness and hence least reactive amongst the members. Importantly, MHP and MEP proved their reliability again.

Stabilization of a species in aqueous phase is well accounted by the magnitude of free energy of solvation, $\Delta G_{sol,aq}$ [52] and to examine the stability of the species in solvent phase, $\Delta G_{sol,aq}$ of the Az^+ ions have been calculated. Trend observed in $\Delta G_{sol,aq}$ is: 1b(−58.66) > 4b(−55.27) > 5b(−53.56) > 3b(−53.27) > 2b(−53.22), values given in brackets are in kcal/mol; large value of $\Delta G_{sol,aq}$ leads to stabilization of the Az^+ ions in aqueous phase. Earlier, we performed calculations on $\Delta G_{sol,aq}$ for some of the nitrogen mustards (mustine, melphalan, chlorambucil, bendamustine, phosphoramide mustard, spiromustine and uracil mustard) and results obtained were ∼−65 kcal/mol (at B3LYP/6-31+G(d) level of theory) [53]. Az^+ ions of the formononetin derivatives too exhibit comparable values of $\Delta G_{sol,aq}$ to that of the other nitrogen mustards.

Earlier, Polavarapu et al. anticipated the free energy of activation for mustine, melphalan and chlorambucil [30]. They observed that melphalan and chlorambucil possess higher free energy of activation compared to mustine (9.26 kcal/mol, 22.53 kcal/mol and 23.00 kcal/mol for mustine, chlorambucil and melphalan, respectively). Free energy of activation of the formononetin nitrogen mustards is of same magnitude as that of chlorambucil or melphalan and we expect that Az^+ ion formation in case of formononetin derivatives are slower compared to mustine, Table 2.

Thus, our observations advocated that the formononetin nitrogen mustards are successful in slowing down the rate of Az^+ ion formation. Importantly, global hardness and global electrophilicity pattern of the drug molecules and their corresponding Az^+ ions follow MHP and MEP. Analysis made on the Az^+ ion formation demonstrates absence of thermodynamic as well as kinetic driving force for the reaction.

4.2. Guanine alkylation

The vital part of guanine alkylation (b → c, Fig. 1) is the C1–N7 bond formation; thus interaction energy between Az^+ ion and guanine as well as thermodynamic and kinetic driving forces of the reaction becomes important. The alkylation reaction passes through a transition state (TS2); a schematic diagram of the transition state in gas phase along with some important structural parameters is summarized in Fig. 4. It has been observed that the transition state geometry in all the drug molecules are very close to each other: C1-N3 bond lengths are ∼1.9 Å, C1–N7 bond lengths are ∼2.1 Å and ∠N3C2C1 bond angles are ∼80°. However, it is important to note that the structural parameters of the Az^+ ion moeity in TS2 are different from that of TS1. A larger ∠N3C2C1 bond angle in TS2 compared to that in TS1 is observed, indicating that the tricyclic Az^+ ring rip apart in TS2, compared to TS1.

Thermodynamic and kinetic aspects of the adduct formation process are examined in terms of free energy of activation ($\Delta G_2^{\dagger}$) and enthalpy (ΔH_2); calculated values in gas and aqueous phase are summarized in Table 3. Free energy of activation ($\Delta G_2^{\dagger}$) for adduct formation is comparatively low to that of Az^+ ion formation in both phases, Table 3. Another interesting observation is that, in case of Az^+ ion formation, we observed a colossal drop in $\Delta G_1^{\dagger}$ on moving from gas to aqueous phase; however, we did not observe such drop in $\Delta G_2^{\dagger}$ values during adduct formation process. Magnitude of gas phase $\Delta G_2^{\dagger}$ for adducts formation lies in the range 16.99–22.20 kcal/mol. The order is: 3b → 3c > 5b → 5c > 1b → 1c > 2b → 2c > 5b → 5c, almost similar trend is observed in aqueous phase. These values are observed to be comparable to the activation barrier of platination of guanine [54]. Interestingly, activation barrier of guanine alkylation by these drug molecules are lower than by ethylene or propylene oxide [55–56]. In addition to alkylating guanine, the aziridinium ion may undergo hydrolysis. Pineda et al. have studied the hydrolysis of a chlorambucil analogue using density functional theory and the results obtained were comparable to the experimental data [57].

In contrast to the Az^+ ion formation, which is endothermic in nature, the adduct formation is observed to be exothermic for all the drug molecules in gas as well as aqueous phase. Enthalpy gain is comparable in all the five cases and observed to be maximum for 1b → 1c, −35.92 kcal/mol and minimum in case of 4b → 4c, −34.16 kcal/mol, Table 3. Aqueous phase results demonstrates the importance of polar solvent on the thermochemistry of the drug-guanine adduct formation process; subsequently we observed a decrease in $\Delta G_2^{\dagger}$ and ΔH_2 values in aqueous phase by ∼5 kcal/mol; role of polar solvent cannot be ruled out. Our results reveal the existence of a strong thermodynamic driving force for the investigated drug-guanine adducts formation compared to mustine, melphalan or chlorambucil [30]. Important to note is that, a smaller free energy of activation in case of adduct formation, compared to Az^+ ion formation, support the existence of kinetic driving force for adduct formation. Interaction energies in gas and aqueous phases are presented in Table 4.

Interaction energy values advocating a strong interaction between the Az^+ ion and guanine moiety; magnitude of interaction energy is ∼−10 kcal/mol in gas phase; however, incorporation of aqueous phase doubled the interaction energy, Table 4. Results proved the immense role of aqueous phase on interaction energy. Interaction energies confirmed formation of a stable mono-adduct, which in turn contributes to the genotoxicity of the drug molecules.

Stability of drug-guanine adducts are examined form their global hardness and global philicity (1c–5c) in both gas and aqueous

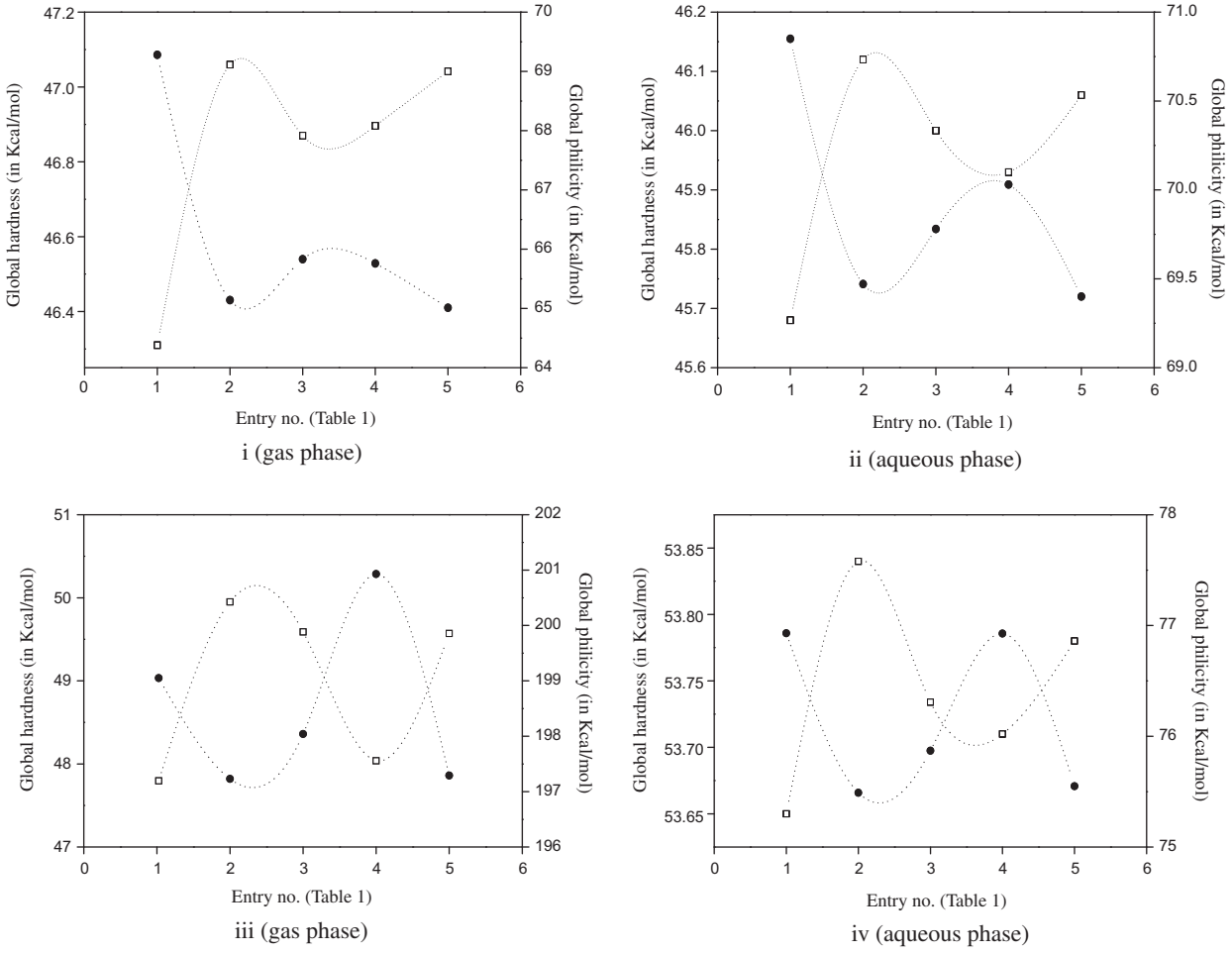

Fig. 3. Global hardness (η) and global electrophilicity (ω) of drug molecules (i and ii) and Az^{+} ions (iii and iv) of the drug molecule in gas and aqueous phase at B3LYP/6-31G(d,p) level of theory. (● Global electrophilicity, □ global hardness).

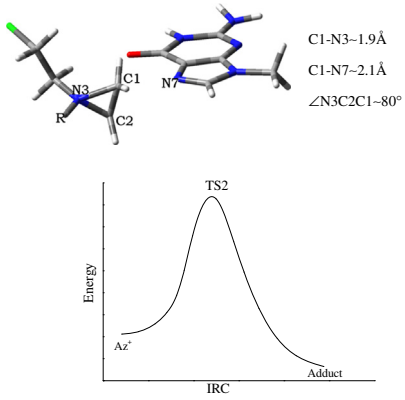

Fig. 4. Schematic diagram of the transition state involved in guanine alkylation (TS2, b → c).

phases, Fig. 5. Both gas and aqueous phase results show similar trends. Importantly, 3c exhibits least hardness in both phases implying formation of least stable adduct (η = 26.86 kcal/mol in gas phase and 45.12 kcal/mol in aqueous phase) and 1c is the most stable adduct (in accordance with MHP, η = 32.57 kcal/mol in gas phase and 49.55 kcal/mol in aqueous phase) among the drug molecules. We expect that the least stable adduct '3c' would play its part in further reaction i.e. formation of cross-linked adduct at an ease compared to the other members. Fig. 5 confirmed the validity of the MHP and MEP.

Table 3
Free energy of activation ($\Delta G_2^{\dagger}$) and enthalpy (ΔH_2) involved in drug-guanine adduct formation (b → c) in gas and aqueous phase (values are in kcal/mol).

Step	$\Delta G_2^{\dagger}$		ΔH_2	
	Gas phase	Aqueous phase	Gas phase	Aqueous phase
1b → 1c	19.68	16.20	−35.92	−30.30
2b → 2c	18.89	14.53	−34.60	−28.57
3b → 3c	22.20	17.08	−35.37	−29.34
4b → 4c	16.99	13.07	−34.16	−28.13
5b → 5c	20.80	16.00	−35.50	−29.36

Table 4
Interaction energies (ΔE_{int}) in drug-guanine adducts in gas and aqueous phase (values are in kcal/mol).

Step	Gas phase	Aqueous phase
1b → 1c	−10.88	−21.29
2b → 2c	−10.57	−21.23
3b → 3c	−11.88	−23.22
4b → 4c	−10.61	−21.18
5b → 5c	−12.13	−21.68

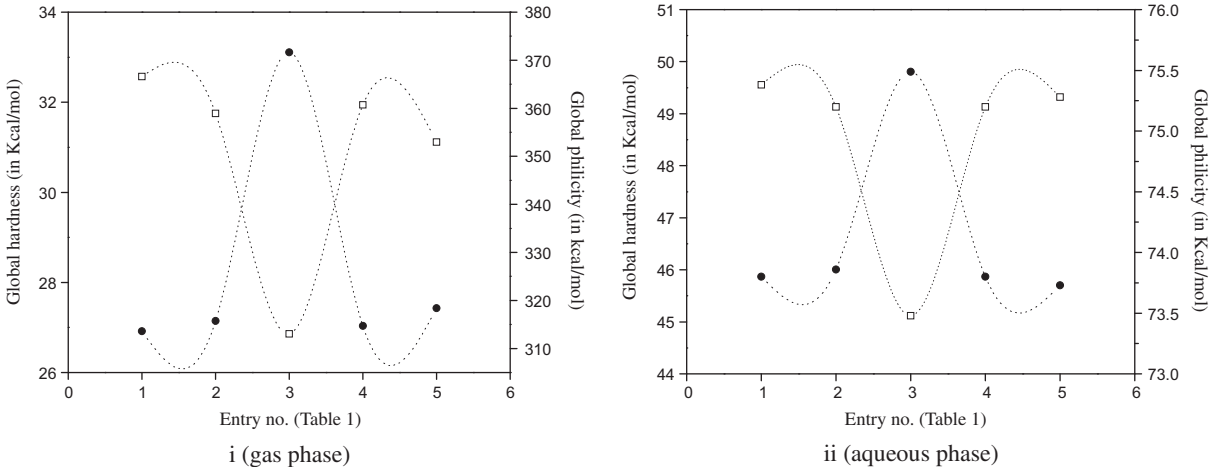

Fig. 5. Global hardness and global electrophilicity of the drug-guanine adducts in gas and aqueous phase at B3LYP/6-31G(d,p) level of theory. (● Global electrophilicity, □ global hardness).

5. Conclusion

We studied the kinetic and thermodynamic aspects of Az^+ ion formation and guanine alkylation by five derivatives of formononetin nitrogen mustard. Both the processes pass through a transition state. Investigated results authenticate that the rate of Az^+ ion formation by the derivatives of formononetin nitrogen mustard is quite sluggish compared to that of mustine. Low energy barrier of the drug-guanine adduct formation over Az^+ ion formation provided an evidence of the former being kinetically more favoured. Similarly, conclusion drawn from thermodynamic studies suggest that the thermodynamic driving force is against the motion in case of Az^+ ion formation but is for the motion in case of drug-guanine adducts formation. Due to formation of the charged species (Az^+ and Cl^-) in the first step of the reaction, aqueous phase exerts larger impact on Az^+ ion formation, however, such effect is not observed in case of drug-guanine adduct formation. This suggests that solvent phase free energy of activation is more important for reactions that involve formation of charged species. Free energy of activation of Az^+ ion and adduct formation by formononetin nitrogen mustard derivatives are comparable to those of chlorambucil or melphalan [30]. Free energy of solvation of Az^+ ions advocates the stability of the species in aqueous phase.

Acknowledgement

Authors acknowledges the financial support from Department of Science and Technology, DST, (SR/S1/PC-13/2009), New Delhi.

References

[1] S.R. Rajski, R.M. Williams, DNA Cross-Linking Agents as Antitumor Drugs, Chem. Rev. 98 (1998) 2723–2795.
[2] P.D. Lawley, Alkylation DNA Aftermath, BioEssays 17 (1995) 561–568.
[3] D.M. Noll, T.M. Mason, P.S. Miller, Formation and repair of interstrand cross-links in DNA, Chem. Rev. 106 (2006) 277–301.
[4] P. Rhoads, Nitrogen mustards in the treatment of neoplastic disease, J. Am. Med. Assoc. 131 (1946) 656–658.
[5] C.M. Haskel, Cancer Treatment, second ed., Saunders, Philadelphia, 1990.
[6] B.J. Sanderson, A.J. Shield, Mutagenic damage to mammalian cells by therapeutic alkylating agents, Mutat. Res. 355 (1996) 41–57.
[7] K.W. Kohn, in: H. Tapiero, J. Robert, T.J. Lampidis (Eds.), Anticancer Drugs, INSERM, John Libbley Eurotext, London, Paris, 1989.
[8] L.O. Jacobson, C.L. Spurr, Studies on the effect of methyl bis (beta-chloroethyl) amine hydrochloride on diseases of the hemopoietic system, J. Clin. Invest. 25 (1946) 909.
[9] A. Gilman, F.S. Philips, The biological actions and therapeutic applications of the b-chloroethyl amines and sulfides, Science 103 (1946) 409–415.
[10] L.S. Goodman, M.M. Wintrobe, W. Dameshek, M.J. Goodman, A. Gilman, M.T. McLennan, Nitrogen mustard therapy: use of methyl-bis(beta-chloroethyl)amine hydrochloride and tris(beta-chloroethyl)amine hydro chloride for hodgkin's disease, lymphosarcoma, leukemia and certain allied and miscellaneous disorders, J. Am. Med. Assoc. 132 (1946) 126–132.
[11] H. Borch, A. Hamza, D. Vasilescu, Ab initio modeling of the interaction between Guanine – Cytosine pair and mustard alkylating agents, Quantum Biol. Symp. 60 (1996) 1745–1764.
[12] K.W. Kohn, J.A. Hartley, W.B. Mattes, Mechanisms of DNA sequence selective alkylation of guanine-N7 positions by nitrogen mustards, Biochem. Pharmacol. 37 (1988) 1799–1800.
[13] S.M. Rink, M.S. Solomon, M.J. Taylor, R.B. Sharanabasava, L.W. McLaughlin, P.B. Hopkins, Covalent structure of a nitrogen mustard-induced DNA interstrand cross-link: an N7-to-N7 linkage of deoxyguanosine residues at the duplex sequence 5′-d(GNC), J. Am. Chem. Soc. 115 (1993) 2551–2557.
[14] P. Calabresi, R.E. Parks, A. Gilman, L.S. Goodman, T.W. Raol, in: F. Murad (Ed.), The Pharmacological Basis of therapeutics, Macmillan, New York, 1985.
[15] B. Singer, The chemical effects of nucleic acid alkylation and their relation to mutagenesis and carcinogenesis, Nature 264 (1976) 333–339.
[16] L.F. Provirk, D.E. Shuker, DNA damage and mutagenesis induced by nitrogen mustards, Mutat. Res. 318 (1994) 205–226.
[17] A. Pullman, B. Pullman, Molecular electrostatic potential of the nucleic acids, Int. J. Quant. Chem. 14 (1981) 289–380.
[18] P.K. Shukla, P.C. Misra, S. Suhai, Reactions of DNA bases with the anti-cancer nitrogen mustard mechlorethamine: a quantum chemical study, Chem. Phys. Lett. 449 (2007) 323–328.
[19] B. Singer, The chemical effects of nucleic acid alkylation and their relation to mutagenesis and carcinogenesis, Prog. Nucl. Acids Res. Mol. Biol. 15 (1975) 219–284.
[20] M.R. Osborne, D.E.V. Wilman, P.D. Lawley, Alkylation of DNA by the nitrogen mustard bis(2-chloroethyl)methylamine, Chem. Res. Toxicol. 8 (1995) 316–320.
[21] P.D. Lawley, Effects of some chemical mutagens and carcinogens on nucleic acids, Prog. Nucl. Acids Res. Mol. Bimol. 5 (1966) 89–131.
[22] R.B. Silverman, The Organic Chemistry of Drug Design and Drug Action, Elsevier Scademic Press, USA, 2004.
[23] B. Marvania, P.C. Lee, R. Chaniyara, H. Dong, S. Suman, R. Kakadiya, T.C. Chou, T.C. Lee, A. Shah, T.L. Su, Synthesis and antitumor evaluation of phenyl n-mustard-quinazoline conjugates, Biorg. Med. Chem. 15 (2011) 1987–1998.
[24] P.G. Baraldi, R. Romagnoli, P.M. Giovanna, C.N.M. Del, J.P. Bingham, J.A. Hartley, Benzoyl and cinnamoyl nitrogen mustard derivatives of benzoheterocyclic analogues of thetallimustine: synthesis and antitumor activity, Bioorg. Med. Chem. 10 (2002) 1611–1618.
[25] P.G. Baraldi, I. Beria, P. Cozzi, C. Geroni, A. Espinosa, M.A. Gallo, A. Entrena, J.P. Bingham, J.A. Hartley, R. Romagnoli, Cinnamoyl nitrogen mustard derivatives of pyrazole analogues of tallimustine modified at the amidino moiety: design, synthesis, molecular modeling and antitumor activity studies, Bioorg. Med. Chem. 12 (2004) 3911–3921.
[26] T.-L. Su, Y.-W. Lin, T.-C. Chou, X. Zhang, V.A. Bacherikov, C.-H. Chen, L.F. Liu, T.-J. Tsai, Potent antitumor 9-anilinoacridines and acridines bearing an alkylating N-mustard residue on the acridine chromophore: synthesis and biological activity, J. Med. Chem. 49 (2006) 3710–3718.
[27] N. Kapuriya, K. Kapuriya, X. Zhang, T.-C. Chou, R. Kakadiya, Y.-T. Wu, T.-H. Tsai, Y.-T. Chen, T.C. Lee, A. Shah, Y. Naliapara, T.-L. Su, Synthesis and biological activity of stable and potent antitumor agents, aniline nitrogen mustards

linked to 9-anilinoacridines via a urea linkage, Bioorg. Med. Chem. 16 (2008) 5413–5423.
[28] J. Ren, H.-J. Xu, H. Cheng, W.-Q. Xin, X. Chen, K. Hu, Synthesis and antitumor activity of formononetin nitrogen mustard derivatives, Eur. J. Med. Chem. 54 (2012) 175–187.
[29] D.J. Mann, Aziridinium ion ring formation from nitrogen mustards: mechanistic insights from Ab initio dynamics, J. Phys. Chem. A 114 (2010) 4486–4493.
[30] A. Polavarapu, J.A. Stillabower, S.G.W. Stubblefield, W.M. Taylor, M.H. Baik, The mechanism of guanine alkylation by nitrogen mustards: a computational study, J. Org. Chem. 77 (2012) 5914–5921.
[31] (a) T. Mineva, T. Heine, Efficient computation of orbitally resolved hardness and softness within density functional theory, J. Phys. Chem. A. 108 (2004) 11086–11091;
(b) G. Molteni, A. Ponti, Arylazide cycloaddition to methyl propiolate: DFT-based quantitative prediction of regioselectivity, Chem. Eur. J. 9 (2003) 2770–2774;
(c) R.K. Roy, Nucleophilic substitution reaction of alkyl halides: a case study on density functional theory (DFT) based local reactivity descriptors, J. Phys. Chem. A 107 (2003) 397–404;
(d) P.K. Chattaraj, S. Sengupta, Popular electronic structure principles in a dynamical context, J. Phys. Chem. 100 (1996) 16126–16130.
[32] (a) P. Geerlings, F.D. Proft, W. Langenaeker, Conceptual density functional theory, Chem. Rev. 103 (2003) 1793–1873;
(b) P.K. Chattaraj, U. Sarkar, D.R. Roy, Electrophilicity index, Chem. Rev. 106 (2006) 2065–2091.
[33] P.K. Chattaraj, S. Nath, B. Maiti, in: J. Tollenaere, P. Bultinck, H.D. Winter, W. Langenaeker (Eds.), Computational medicinal chemistry and drug discovery, Marcel Dekker, New York, 2003.
[34] R.G. Parr, Density functional theory, Annu. Rev. Phys. Chem. 34 (1983) 631–656.
[35] R.G. Parr, W. Yang, In Density Functional Theory of Atoms and Molecules, Oxford University Press, New York, 1989.
[36] R.G. Parr, L.V. Szentpaly, S. Liu, Electrophilicity index, J. Am. Chem. Soc. 121 (1999) 1922–1924.
[37] R.G. Pearson, Chemical Hardness–Applications from Molecules to Solids, VCH-Wiley, Weinheim, 1997.
[38] R.G. Parr, R.A. Donnelly, M. Levy, W.E. Palke, Electronegativity: the density functional viewpoint, J. Chem. Phys. 68 (1978) 3801–3807.
[39] R.G. Parr, R.G. Pearson, Absolute hardness: companion parameter to absolute electronegativity, J. Am. Chem. Soc. 105 (1983) 7512–7516.
[40] R.G. Pearson, Absolute electronegativity and absolute hardness of Lewis acids and bases, J. Am. Chem. Soc. 107 (1985) 6801–6806.
[41] T.A. Koopmans, Über die Zuordnung von Wellenfunktionen und Eigenwerten zu den einzelnen Elektronen eines Atoms, Physica 1 (1933) 104–113.
[42] A.D. Becke, Density-functional exchange-energy approximation with correct asymptotic behavior, Phys. Rev. A 38 (1988) 3098–3100.
[43] C.T. Lee, W.T. Yang, R.G. Parr, Development of the colle-salvetti correlation-energy formula into a functional of the electron-density, Phys. Rev. B 37 (1988) 785–789.
[44] H.B. Schlegel, in: Yarkony (Ed.), Geometry Optimization on Potential Energy Surfaces, In Modern Electronic Structure Theory, World Scientific Publishing, Singapore, 1994.
[45] (a) B. Mennucci, J. Tomasi, Continuum solvation models: a new approach to the problem of solute's charge distribution and cavity boundaries, J. Chem. Phys. 106 (1997) 5151–5198;
(b) S. Miertus, E. Scrocco, J. Tomasi, Electrostatic interaction of a solute with a continuum – a direct utilization of abinitio molecular potentials for the prevision of solvent effects, J. Chem. Phys. 55 (1981) 117–129.
[46] V. Marenich, C.J. Cramer, D.G. Truhlar, Universal solvation model based on solute electron density and a continuum model of the solvent defined by the bulk dielectric constant and atomic surface tensions, J. Phys. Chem. B 113 (2009) 6378–6396.
[47] Gaussian 09, Revision B.01, Gaussian Inc., Wallingford CT, 2010.
[48] (a) R.G. Pearson, Recent advances in the concept of hard and soft acids and bases, J. Chem. Edu. 64 (1987) 561–570;
(b) R.G. Pearson, The principle of maximum hardness, Acc. Chem. Res. 26 (1993) 250–255.
[49] C. Morell, V. Labet, A. Grand, H. Chermette, Minimum electrophilicity principle: an analysis based upon the variation of both chemical potential and absolute hardness, Phys. Chem. Chem. Phys. 11 (2009) 3417–3423.
[50] B. Neog, N. Sarmah, R. Kar, P.K. Bhattacharyya, Effect of external electric field on aziridinium ion intermediate: a DFT study, Comput. Theor. Chem. 976 (2011) 60–67.
[51] P.K. Bhattacharyya, R. Kar, Does structural variation in the aziridinium ion facilitate alkylation?, Comput Theor. Chem. 967 (2011) 5–11.
[52] M.D. Tissandier, K.A. Cowen, W.Y. Feng, E. Gundlach, M.H. Cohen, A.D. Earhart, T.R. Tuttle, J.V. Coe, The proton's absolute aqueous enthalpy and gibbs free energy of solvation from cluster ion solvation data, J. Phys. Chem. A 102 (1998) 9308.
[53] B. Neog, S. Sinha, P.K. Bhattacharyya, Alkylation of DNA by nitrogen mustards: a DFT study, Comput. Theor. Chem. 1018 (2013) 19–25.
[54] M.H. Baik, R.A. Friesner, S.J. Lippard, Theoretical study of cisplatin binding to purine bases: Why does cisplatin prefer guanine over adenine?, J Am. Chem. Soc. 125 (2003) 14082–14092.
[55] A. Kranjc, J. Mavri, Guanine alkylation by ethylene oxide: calculation of chemical reactivity, J. Phys. Chem. A 110 (2006) 5740–5744.
[56] J. Mavri, Can the chemical reactivity of an ultimate carcinogen be related to its carcinogenicity? An application to propylene oxide, Toxicol. in Vitro 27 (2013) 479–485.
[57] F.P. Pineda, J.O. Castro, J.R.A. Idaboy, J. Frau, B.M. Cabrera, J.C. Ramirez, J. Donoso, F. Munoz, Hydrolysis of a chlorambucil, analogue. A density functional study, J. Phys. Chem. A 115 (2011) 2359–2366.